Draft, March 15, 1999

The Origin of Lüders' Bands in Deformed Rock

William A. Olsson
Sandia National Laboratories, Albuquerque, New Mexico

DISCLAIMER

Abstract

Lüders' bands are shear deformation features commonly observed in rock specimens that have been deformed experimentally in the brittle-ductile transition regime. For specimens that contain both faults (shear fractures that separate the specimen) and bands, the bands form earlier in the deformation history and their orientations are often different from the fault. These differences pose the question of the relationship between these two structures. Understanding the origin of these features may shed light on the genesis of apparent natural analogues, and on the general process of rock deformation and fracture in the laboratory. This paper presents a hypothesis for the formation of Lüders' bands in laboratory specimens based on deformation localization theory considered in the context of the nonuniform stress distribution of the conventional triaxial experiment. Lüders' bands and faults appear to be equivalent reflections of the localization process as it is controlled by nonuniform distributions of stress and evolution of incremental constitutive parameters resulting from increasing damage. To relate conditions for localization in laboratory specimens to natural settings, it will be necessary to design new experiments that create uniform stress and deformation fields, or to extract constitutive data indirectly from standard experiments using computational means.

1. Introduction

From the very beginning of modern experimental rock deformation [*von Kármán*, 1911], experimentalists have been recording the occurrence of fine lines on the surfaces of many of their deformed specimens. Oftentimes, there were two intersecting sets of subparallel traces creating a network of lines on the surfaces of the specimens. When two sets were present, their normals were symmetrically disposed about the axis of maximum compression. *Griggs* [1936] was apparently the first to identify these features with the Lüders' lines observed in deformed specimens of metals. In an experimental study that specifically addressed Lüders' lines in rock, *Friedmán and Logan* [1973] gave a detailed description of them for a fine-grained limestone and a sandstone. They modified the term to Lüders' "bands" and this term will be used in this paper. *Friedman and Logan* [1973] defined Lüders' bands as "planar features oriented parallel to planes of high shear stress along which cataclasis is concentrated and shear displacement is negligible." Evidently, these structures can be found in several different rock types so long as the confining pressure is sufficient to bring the deformational response near to the brittle-ductile transition regime as defined by *Heard* [1960]. *Paterson* [1957] interpreted certain tectonic scale fracture zones as Lüders' bands. Some additional studies that either have commented on such features explicitly, or have indicated their existence with photographs of deformed specimens are: *Bredthauer* [1957], *Paterson* [1958], *Wawersik and Fairhurst* [1970], *Donath et al.* [1971], *Hugman and Friedman* [1979] and *Fredrich et al.* [1989].

In experimentally deformed specimens, Lüders' bands are thin (often about 1 mm) and show little or no offset when observed with the unaided eye. Microscopically, they are tabular zones of cataclastic deformation. At the outcrop scale, similar features in sandstone are called deformation bands [*Aydin and Johnson*, 1983] or microfaults [*Jamison and Stearns*, 1982] and exhibit shear displacements of up to a few centimetres. The apparent similarity of Lüders' bands in laboratory specimens to deformation bands and microfaults in the outcrop led *Friedman and Logan* [1973] to suggest that in situ conditions of deformation could be estimated for the outcrop features. In their experiments, *Friedman and Logan* [1973] found that for fine-grained Solenhofen limestone the Lüders' bands were confined to the surface layer of the specimens, but in coarser grained limestone, and sometimes in a sandstone, they were pervasive. Further, in all cases, the bands were best developed where the barrelling of the specimen was greatest. In other words, where the tangential normal strains (stretching) normal to the direction of maximum compression were greatest (Figure 1). They found that for specimens whose cross-sections normal to the maximum shortening direction (originally circular) became elliptical, leading to an orthorhombic deformation pattern, the common line of intersection of the bands with the fault paralleled the short ellipse axis (Figure 1b). *Friedman and Logan* [1973] also found that the angle between the Lüders' band normal and the direction of the maximum compressive stress, σ_1, was less than the angle between the fault normal and σ_1. The maximum, intermediate, and minimum principal compressive stresses are, respectively, σ_1, σ_2, and σ_3.

An orthorhombic symmetry (Figure 1b) is associated with conjugate faults or Lüders' bands; specimens which develop only one set of Lüders' bands or one fault take on a monoclinic symmetry (Figure 1c). My own observations in marble [*Olsson and Peng*, 1976] and sandstone (unpublished) indicate that when a specimen takes on an orthorhombic or monoclinic symmetry there are markedly fewer Lüders' bands on the those parts of the outer surface pierced by the maximum ellipse axis. Further clues to the origin of the bands [*Friedman and Logan*, 1973] are that their orientations are insensitive to axial strain and strain rate, but are influenced by the confining pressure.

In experimental studies [*Wawersik et al.*, 1990; *Olsson*, 1992] designed to test some predictions of the Rudnicki-Rice theory of strain localization [*Rudnicki and Rice*, 1975], Lüders' bands were observed in Tennessee marble. Prisms had been deformed in plane strain, and solid and hollow cylinders had been deformed in axisymmetric compression, and, though bands were present in many specimens, they were not described in the initial reports [*Wawersik et al.*, 1990; *Holcomb*, 1992; *Olsson*, 1992]. Earlier work [*Olsson and Peng*, 1976] had shown that the internal structure of similar bands observed in specimens of Tennessee marble tested in conventional triaxial compression consisted of complex combinations of calcite deformation twins and transgranular and grain-boundary cracks.

The coexistence of faults and Lüders' bands in the same specimen broaches the question of just which of these two shear deformation features is supposed to be predicted by localization theory: the more or less numerous Lüders' bands or the faults that eventually divided that specimen? These structures are both obviously shear strain localizations, but they occur at different stages in the axial shortening and they often have different orientations with respect to the applied stresses. It is evident from these observations that neither the genesis of Lüders' bands nor their relationship to the final fault are yet completely understood.

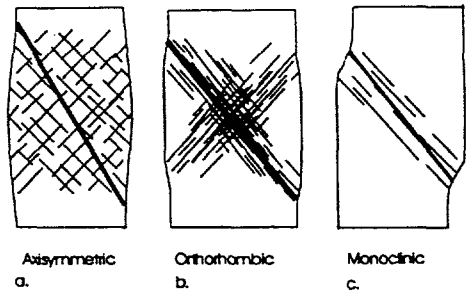

Figure 1. Two-dimensional representations of some typical deformation modes in triaxially deformed specimens. Heavy lines are faults, or shear fractures, that separate the specimens; thin lines are Lüders' bands. In *a*, the Lüders' bands are distributed uniformly around the surface; in *b* and *c*, most Lüders' bands normals occur in the surface lying in the plane of the paper. The dips of the fault and the Lüders' bands can be significantly different in *a*, and the same or nearly the same in *b* and *c*.

Summarizing the points that need to be addressed to better understand the formation of Lüders' bands in the laboratory, and to enable us to extend that understanding to field problems: (1) Lüders' bands form at less specimen shortening than faults; (2) in many cases Lüders' band normals are more steeply inclined to the applied maximum compressive stress than are fault normals; (3) the strikes of the Lüders' bands are most often distributed radially about the cylinder axis when the deformation remains axisymmetric, but can be uniformly oriented when the strain is orthorhombic or monoclinic; (4) Lüders' bands invariably show very little shear offset, much less than the fault; (5) Lüders' bands are sometimes only surface features, but in other cases they are seen to be pervasive throughout the thickness of the specimen, and then their strikes are parallel to the strike of the fault rather than radially dispersed around the cylinder axis; (6) when the bands are pervasive, some faults appear to be simply the concentration of shear along one or more closely spaced Lüders' bands until the offset is so large as to be considered a fault.

2. Hypothesis

I propose that the origin of Lüders' bands in axisymmetrically-deformed laboratory specimens can be understood by considering the conditions for the onset of localization [*Rudnicki and Rice*, 1975] as they are influenced by the local states of stress in a typically inhomogeneously deformed specimen. It should be noted that before inelastic deformation sets in, the state of stress in an axisymmetrically-compressed, elastic cylinder with typical end conditions is nonuniform [*Peng*, 1971; *Al-Chalabi and Huang*, 1974].

The first part of the hypothesis assumes that the localization of deformation is tantamount to a bifurcation from an initially uniform deformation-rate field in accordance with the theory of *Rudnicki and Rice* [1975]. Their calculations were based on a stress-strain relation for constant mean stress that contained the incremental constitutive parameters: the tangent plastic modulus h of the shear stress-strain curve (Figure 2a), shear modulus G, and Poisson's ratio ν. The parameters G and ν have initially their elastic values, but evolve during deformation beyond the yield point. Also included in the

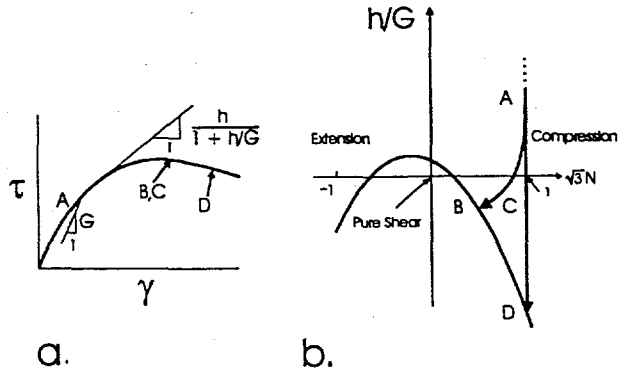

Figure 2. (*a*) Shear stress-strain curve showing the relation between elastic modulus G and plastic modulus h. (*b*) The critical hardening modulus plotted against N, the parameter defining the state of stress. Letters A, B, C and D correspond to key points during deformation of a conventional triaxial specimen; see text for explanation. Redrawn from Figures 3 and 6 of *Rudnicki and Rice* [1975].

description were the ratio of inelastic volume strain increment to inelastic shear strain increment β (the dilatancy), and the local slope of the yield condition μ. *Rudnicki and Rice* [1975] defined the onset of localization in terms of the critical value of the tangent modulus, h_{cr}, normalized by G. They found that the state of stress had a profound influence on the amount of deformation preceding bifurcation, and to present their data they defined a single parameter N to characterize the anisotropy of the stress state. N is defined by $\sigma_2' = N\bar{\tau}$ where the effective shear stress $\bar{\tau}$ is

$$\bar{\tau} = \sqrt{\frac{1}{2}\sigma_{ij}'\sigma_{ij}'}$$

and the prime indicates deviatoric values given by $\sigma_{ij}' = \sigma_{ij} - \sigma_{kk}\delta_{ij}$. The summation convention is used here. The stress state parameter $N = 1/\sqrt{3}$ for $\sigma_1 > \sigma_2 = \sigma_3$, axisymmetric compression; $N = -1/\sqrt{3}$ for $\sigma_1 = \sigma_2 > \sigma_3$, axisymmetric extension.

The tangent modulus at localization h_{cr} is related to N

through (Figure 2b)

$$\frac{h_{cr}}{G} = \frac{(1+\nu)}{9(1-\nu)}(\beta-\mu)^2 - \frac{1+\nu}{2}\left(N + \frac{\beta+\mu}{3}\right)^2 \quad (1)$$

The angle between the normal to the deformation band and the σ_1-direction, θ, is also a function of N and is given by [*Rudnicki and Olsson*, 1998]

$$\theta = \frac{\pi}{4} + \frac{1}{2}\arcsin\alpha \quad (2)$$

where

$$\alpha = \frac{\frac{2}{3}(1+\nu)(\beta+\mu) - N(1-2\nu)}{\sqrt{4-3N^2}} \quad (3)$$

Thus, the critical modulus and shear band angle are seen to be strong functions of the stress state and these relations are illustrated in Figures 2b, 3, and 4. According to the theory, in the absence of vertex hardening, h_{cr}/G at localization in axisymmetric compression has a relatively large negative value. For smaller values of N, closer to pure shear, the critical modulus is larger, and will be positive over a range of stress-state values, unless $\beta = \mu$, in which case h_{cr}/G is never positive. The modulus becomes negative again for states of stress near (axisymmetric) triaxial extension.

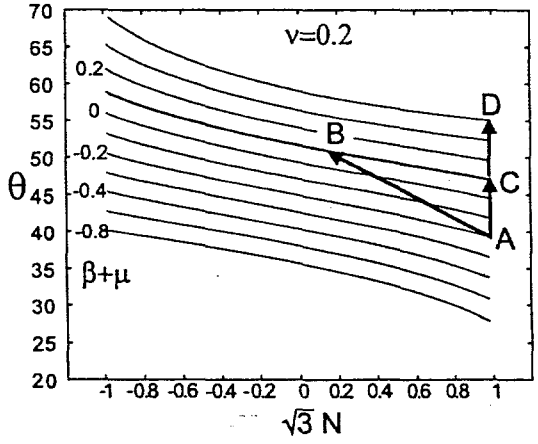

Figure 3. Curves of critical θ for various values of $\beta+\mu$ and $\nu = 0.2$. The heavy arrows show state paths for the central core (ACD) and outer annulus (AB) of a specimen undergoing axial shortening.

Experimental work by *Wawersik et al.*, [1990] on Tennessee marble and by *Ord et al.* [1991] on Gosford sandstone supports the prediction of the model that plane-strain states promote earlier localization, actually occurring pre-peak ($h > 0$) compared to the axisymmetric stress-strain curve. Further, *Olsson* [1992] showed that a vertex formed at the current stress point on the yield surface (or on the plastic potential surface) for Tennessee marble, and according to *Rudnicki and Rice* [1975] this will also allow localization to occur earlier, but still with negative modulus for N near the axisymmetric state.

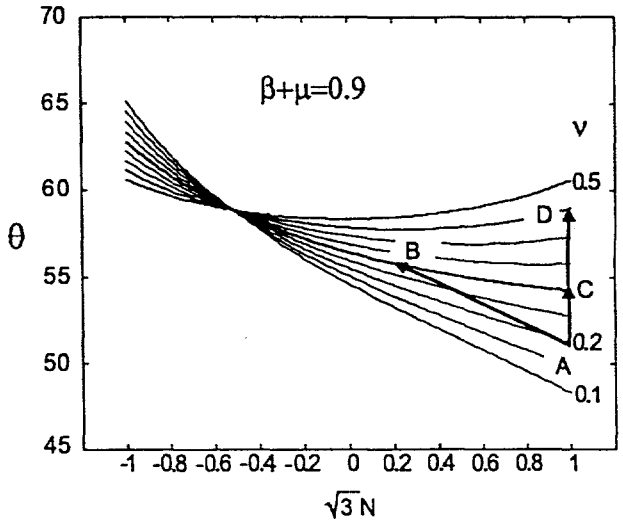

Figure 4. Curves of critical θ for various values of ν and $\beta+\mu = 0.9$. The heavy arrows show state paths for the central core (ACD) and outer annulus (AB) of a specimen undergoing axial shortening.

The second part of the hypothesis requires the development of nonuniform stresses within the specimen. Elastic solutions for a uniaxially loaded cylinder [*Peng*, 1971; *Al-Chalabi and Huang*, 1974] with boundary conditions similar to those in rock deformation experiments show that the stress distributions within the cylinder can be quite nonuniform. Numerical modelling indicates that this nonuniformity in stress that begins during the elastic loading regime likely continues as inelasticity caused by microcracking begins [*Costin and Stone*, 1986; 1987]. In particular, for uniaxial loading of a cylinder, and principal stresses $\sigma_z, \sigma_r, \sigma_\theta$, the hoop stress σ_θ is negative in the cylinder's mid-section. The lowest (most negative) value occurs in the outer annulus. The radial stress σ_r is also negative, but its greatest concentration is less and is near the center of the cylinder. Superposition of a radial confinement may prevent σ_θ from becoming tensile, but, nonetheless, the ratio of σ_θ/σ_r at the outer surface decreases from unity. Therefore, even though a globally axisymmetric load is applied, the material in the outer shell of the mid-section of the cylinder is actually in a true triaxial state of stress such that $\sigma_z > \sigma_r > \sigma_\theta$ (Figure 5). In other words, locally the axial stress σ_z remains the maximum compressive stress, but the tangential stress σ_θ becomes the minimum

compressive stress, and the radial stress σ_r becomes the intermediate compressive stress.

The sequence of formation and the relative orientations of the Lüders' bands and the fault can be better understood by a detailed examination of Figures 2, 3 and 4. These figures are based on similar ones in *Rudnicki and Rice* [1975] and *Rudnicki and Olsson* [1998], respectively. First assume the simplest possible situation, that in which the specimen retains global axial symmetry (Figure 1a). This constraint is loosened in later discussion. Letters indicating certain points in the deformation history characterized by stress state N, normalized plastic modulus h, and material parameters ν, μ and β, are correlated between Figures 2, 3 and 4.

At the start of inelastic deformation, the stress state is at the yield point A in Figure 2a and 2b. At this time, the plastic deformation is zero and the plastic modulus h is infinite, but h decreases rapidly with ensuing plastic strain. A path representing the change in h/G is sketched in Figure 2b. For an ideal, homogeneous, stress state, N would be constant and with increasing plastic deformation the point representing the stress state and modulus would move down a vertical line ACD (Figure 2b) until it came to the h_{cr}/G curve, indicating the onset of shear banding in axisymmetric compression. In reality, in the outer shell N will deviate from the ideal value and drift toward smaller values. This path (AB in Figure 2b) will also terminate against the h_{cr}/G curve. The stresses at which these two paths intersect the h_{cr}/G curve are determined by the stress-strain curve for the rock (Figure 2a).

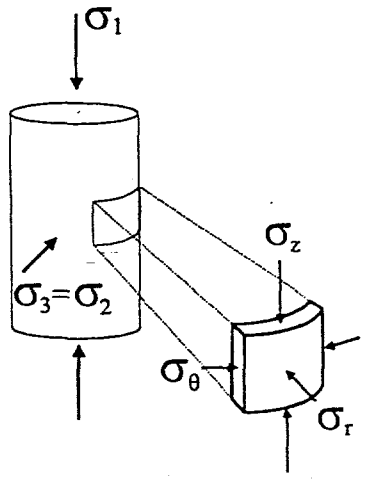

Figure 5. Axisymmetric stress σ_1 and σ_3 are applied to a cylindrical specimen. In the outer annulus these stresses may be modified to $\sigma_z > \sigma_r > \sigma_\theta$ because of the boundary conditions.

In Figure 3, equations (2) and (3) were used to calculate the angles at which any shear bands, either Lüders' bands or faults, will form have been plotted against $\sqrt{3}N$ for $\nu = 0.2$ and various values of $\beta + \mu$. Figure 4 shows a similar plot of θ against $\sqrt{3}N$ for $\beta + \mu = 0.9$ and various values of ν. After application of axial load the stress state is located at a point (A in Figures 2b, 3 and 4) with abscissa $N = 1/\sqrt{3}$ and ordinate determined by the initial elastic values of β, μ and ν. The paths in Figures 2b, 3 and 4 are for illustration and do not represent any actual material. The point A is placed for an arbitrary set of initial properties; different rocks will plot at different points along the ordinate. Beginning with elastic stressing and continuing into the inelastic regime, the state point B for the outer shell moves to the left (Figures 3 and 4) as a result of decreasing σ_θ indicating that the stress state in the outer shell is becoming more anisotropic. For the limit case of inelastic deformation without change in material properties, that is, constant β, μ and ν, the state point would move along the contour containing point A. It is more likely that material properties will change with continuing deformation. Most rocks show increasing values of β and ν with shear strain [*Jaeger and Cook*, 1976] and this is assumed for this discussion.

Variation in μ with with strain hardening during axisymmetric compression can be more complex because it depends on whether the stress path intersects a shear yield curve or a volume yield curve (cap) (Figure 6). Yield caps have been documented for porous sandstones by *Wong et at.* [1992], but are not observed for low porosity rocks at pressures usually attained in the laboratory. (Low porosity rocks are usualy characterized by dilation at failure rather than compaction.) Hardening of the yield surface leads to a family of yield curves whose slope is μ on a plot of $\bar{\tau}$ vs. mean stress. In Figure 6 the thin lines are the initial yield curve shown by $\bar{\tau}_o$ and subsequent yield curves, one of which is indicated by $\bar{\tau}_n$. These are bounded above by the limit surface shown by the heavy line. In general, the limit surface need not be a member of the family of yield surfaces. For most rocks this family of shear yield curves forms a fan diverging to higher mean stress, and therefore, the (axisymmetric) triaxial compression test path will experience increasing values of μ as it crosses successively higher yield curves. The value of μ is indicated at the intersection of a stress path (leftmost, Figure 6) with a shear yield curve and at the intersection of another stress path (rightmost, Figure 6) with the yield cap. Therefore, if the loading stress path intersects the shear yield curve first, μ may be positive and increase slightly during hardening. If the triaxial stress path intersects a yield cap, then during hardening of the cap, μ will first be negative and increase greatly during hardening.

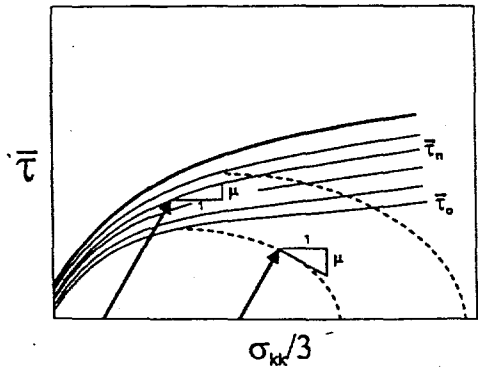

Figure 6. Sketch of typical yield surface (solid curves) and possible yield caps (dashed curves). Heavy arrows represent the stress paths for two triaxial compression tests. See text for expanation.

Considering the likely case of increasing values for each of β, μ and ν, the outer shell state point moves to B (Figures 2b, 3, 4) while the global state, remaining axisymmetric, moves to C. In so doing, the two state paths cross several contours of $\beta + \mu$ (Figure 3) and ν (Figure 4). For ease of discussion it is assumed, but is not necessary, that during the early stages, the material properties vary fairly uniformly throughout the specimen. Thus, the central core of the specimen and the outer shell arrive at different stress states, as indicated by $\sqrt{3}N$, on the same contour of $\beta + \mu$ in Figure 3 or ν in Figure 4. At B, localization occurs in the outer wall because the path in Figure 2b has intersected the critical modulus curve given by (1), which relates h_{cr}/G to β, μ, and ν. This essentially fixes the evolution of material properties in the outer shell because further deformation is mostly accommodated by slip on the surficial shear bands.

Hardening of the first-formed bands may lead to the formation of more bands at higher applied axial deformation. Also, the orientation of the surface bands in the outer shell is henceforth relatively static. What change in angle there may occur at this stage in the axial deformation is due mostly to the geometric rotation caused by shortening of the outer shell. For this special case of global axisymmetric deformation, further deformation moves the overall specimen state to point D (Figure 2, 3 and 4) because of further evolution of material parameters. At D overall localization or faulting can occur because the specimen state now lies on the h_{cr}/G curve at D (Figure 2b). A fault occurs at lower h_{cr}/G and larger global axial shortening (Figure 2), and its normal is at a greater angle to σ_1 than those of the surface shear bands (Figures 3, 4). The angle between the normals to the surface bands and the fault, which here is attributed to material property evolution, may be enhanced very slightly after their formation by the shortening of the specimen which would cause some decreasing of θ for the surface shear bands.

Though $N = 1/\sqrt{3}$ throughout the cylinder at the beginning of application of shear stress, as a result of inhomogenous deformation it inevitably begins to decrease with increasing axial load and the stress state point for the outer shell of material moves from point A toward B (Figures 3 and 4) allowing for earlier localization. It is concluded that in inhomogeneous axisymmetric compression the first shear localization would occur on the surface of the cylinder and be more prevalent in the most bulged regions near the mid-section where σ_θ is reduced to its minimum value, and the state of stress is most anisotropic. Because the tangential stress concentration decays toward the center, these bands will be largely confined to the near-surface. By analogy with strike-slip (mode III deformation) faults, the depth, offset, and length are interrelated, and because the depth is not large, neither are the length nor the offset. The value of the critical modulus h_{cr} and the orientation of the bands is controlled by the local state of stress, and also by the current values of the incremental properties β, ν, and μ. If overall axial symmetry is maintained, the spacing and orientation will be uniform around the specimen; hence, the bearings of the lines of intersection are radially disposed (Figure 1a). If some perturbation in stress, due to imperfection in the end conditions or variation in material properties, is present, a different overall deformation geometry may develop (Figure 1b,c).

This conceptual process can be generalized to arrive at different relationships between Lüders' bands and faults for different deformation symmetries. For example, if the initial boundary conditions are non-axisymmetric, the specimen may take on an orthorhombic symmetry (Figure 1b), and then the surficial strains that coincide with the plane of maximum principal, global strains will be the most anisotropic. They will correspond to the most anisotropic stress state. In this case, the surface strains may be an accurate reflection of the global deformation; therefore, the stress state of the surface, as viewed down the intermediate strain axis (coincident with the strike of the eventual fault), and the stress state of the specimen core may move together from A to B in Figures 2, 3 and 4, undergoing Lüders' banding simultaneously with faulting. This would result in the orientations of the Lüders' bands and the fault being equivalent. In fact, the fault would be nothing more than a shear band with large displacement. The monoclinic symmetry is simply a special case of this one.

3. Discussion

One of the main reasons for studying the origin of Lüders' bands was because *Friedman and Logan* [1973]

suggested that their occurrence may be used to estimate the conditions of formation of apparent natural analogues. They suggested that confining pressure was an important factor and axial strain was not.

It seems clear that the factors that govern the appearance of Lüders' bands are the plastic modulus, state of stress, and the values of the evolving constitutive parameters, ν, μ, and β. In addition to its contribution to the tangential and radial stresses, confining pressure influences the evolution of the constitutive parameters. Contrary to the conclusion of *Friedman and Logan* [1973] axial strain does seem to be involved but its effect is complicated by the details of how the tangential strain and therefore the state of stress develops.

The main problem in using the laboratory test conditions to estimate the in situ conditions of formation is that the local state of stress (in the outer annulus of the specimen) for formation of Lüders' bands is not known; it is often not the applied state of stress. In the case where the specimen takes on a rather two-dimensional deformation pattern, such as here called orthorhombic or monoclinic, the Lüders' bands and faults are the same or nearly the same thing. In those cases the extrapolation of laboratory conditions to field conditions may be a better approximation.

A better way to study the relationship between Lüders' bands and faults would be to develop more uniform stress fields in laboratory specimens. As mentioned earlier, true-triaxial and hollow cylinder configurations seem to show a much better correlation between Lüders' bands and faults [*Wawersik et al.*, 1990; *Olsson*, 1992], that is, they really seem to be the same thing. It may be that if the stress field in a specimen was completely uniform, then only one band could form, starting from a region defined by material property deviations. This suggests that in the field, certain types of stress gradients are necessary for the development of sets of shear bands rather than faults. More work to define whether Lüders' bands occur at all in well-designed experiments seems appropriate.

4. Conclusions

A hypothesis for the formation of Lüders' bands has been presented. It is based on the predictions of the onset of strain localization by the Rudnicki-Rice theory considered within the context of existing solutions for the nonuniform stress state in cylinders subjected to axisymmetric loading. It was concluded that the first strain localization would occur in the outer shell of the cylinder where the stress state is locally non-axisymmetric. The model suggests that Lüders' bands and faults that eventually divide an experimental specimen are both reflections of the same constitutive instability, but arise in different stress and deformation states. According to this hypothesis we may correlate natural analogues (deformation bands) with laboratory Lüders' bands. The problem remaining is to determine the exact state of stress, and constitutive parameter values at the onset of these first localizations. This can be done only through tests that avoid or mitigate nonuniform deformation fields, or indirectly through numerical simulation of conventional axisymmetric experimental data.

It appears that what heretofore have been referred to as Lüders' bands are actually the same phenomenon as faults, that is, they are both shear bands. In actuality, Lüders' bands as usually observed are simply experimental artifacts and result from satisfying the localization condition in stress gradients.

The results of this study indicate that there is a complex interplay between the conditions for localization and the inhomogeneous stress states, common to triaxial testing. Thus, direct estimates of the state of stress associated with strain localization in either triaxial laboratory experiments or in situ situations will be difficult.

Acknowledgments. I thank D. J. Holcomb, J. W. Rudnicki, and D. H. Zeuch for helpful discussions and comments on the manuscript. The support of the U.S. Department of Energy's Office of Basic Energy Sciences/Geosciences and the Office of National Petroleum Technology is gratefully acknowledged. Sandia is a multiprogram laboratory operated by Sandia Corporation, a Lockheed Martin Company, for the United States Department of Energy under contract DE-ACO4-94AL85000.

References

Al-Chalabi, M., and C.L. Huang, Stress distribution within circular cylinders in compression, *Int. J. Rock Mech. Min. Sci., 11*, 45–56, 1974.

Aydin, A., and A. M. Johnson, Analysis of faulting in porous sandstones, *J. Struct. Geol., 5*, 19–31, 1983.

Bredthauer, R. O., Strength characteristics of rock samples under hydrostatic pressure, *Trans. Amer. Soc. Mech. Engrs., 79*, 695–708, 1957.

Costin, L. S., and C. M. Stone, Analysis of triaxial testing using a fracture damage model, in Proc. Soc. Expt. Mech. Spring Conference, New Orleans, 1986.

Costin, L. S., and C. M. Stone, Implementation of a finite element damage model for rock, in *Constitutive Laws for Engineering Materials*, edited by C. S. Desai, E. Krempl, P. D. Kiousis, and T. Kundu, 829–840, Elsevier, New York, 1987.

Donath, F. A., R. T. Faill, and D. G. Tobin, Deformational mode fields in experimentally deformed rock, *Geol. Soc. Amer. Bull., 82*, 1441–1462, 1971.

Fredrich, J. T., B. Evans, and T.-f. Wong, Micromechanics of the brittle to plastic transition in Carrara Marble, *J. Geophys.*

Donath, F. A., R. T. Faill, and D. G. Tobin, Deformational mode fields in experimentally deformed rock, *Geol. Soc. Amer. Bull., 82*, 1441–1462, 1971.

Fredrich, J. T., B. Evans, and T.-f. Wong, Micromechanics of the brittle to plastic transition in Carrara Marble, *J. Geophys. Res., 94*, 4129-4145, 1989.

Friedman, M., and J. M. Logan, Lüders' bands in experimentally deformed sandstone and limestone, *Geol. Soc. Amer. Bull., 84*, 1465–1476, 1973.

Heard, H. C., Transition from brittle fracture to ductile flow in Solenhofen limestone as function of temperature, confining pressure, and interstitial fluid pressure, in *Geol. Soc. Amer. Memoir, 79*, 193–226, edited by D. Griggs and J. Handin, 1960.

Holcomb, D. J., Localization studies under triaxial conditions, in *Proc. 33rd U. S. Symposium on Rock Mech.*, edited by J. R. Tillerson and W. R. Wawersik, 661–670, Balkema, Brookfield, 1992.

Hugman, R. H. H., III, and M. Friedman, Effects of texture and composition on mechanical behavior of experimentally deformed carbonate rocks, *Amer. Assoc. Petrol. Geologists Bull., 63*, 1478–1489, 1979.

Jaeger, J.C., and N.G.W. Cook, *Fundamentals of Rock Mechanics*, 2nd ed., John Wiley and Sons, New York, 1976.

Jamison, W.R., and D.W. Stearns, Tectonic deformation of Wingate sandstone, Colorado National Monument, *Bull. Amer. Assoc. Petrol. Geol., 66*, 2584–2608, 1982.

Kármán, T. von, Festigkeitsversuche unter allseitigem Druck., *Z. Verein. Dtsch. INg., 55*, 1749–1757, 1911.

Olsson, W. A., The formation of a yield-surface vertex in rock, in *Proc. 33rd U. S. Symposium on Rock Mech.*, edited by J. R. Tillerson and W. R. Wawersik, 701–705, Elsevier, Brookfield, 1992.

Olsson, W. A., and S. S. Peng, Microcrack nucleation in marble, *Int. J. Rock Mech. Min. Sci., 13*, 53–59, 1976.

Ord, A., I. Vardoulakis, and R. Kajewski, Shear band formation in Gosford sandstone, *Int. J. Rock Mech. Min. Sci., 28*, 397–409, 1991.

Paterson, M. S., Lüders' bands and plastic deformation in the Earth's crust, *Bull. Geol. Soc. Amer., 68*, 129–130, 1957.

Paterson, M. S., Experimental deformation and faulting in Wombeyan marble, *Geol. Soc. Amer. Bull., 69*, 465–476, 1958.

Peng, S. D., Stresses within elastic circular cylinders loaded uniaxially and triaxially, *Int. J. Rock Mech. Min. Sci., 8*, 399–432, 1971.

Rudnicki, J. W., and W. A. Olsson, Re-examination of fault angles predicted by shear localization theory, NARMS '98, paper no. 512, *Int. J. Rock Mech. Min. Sci. 35*, 1998.

Rudnicki, J. W., and J. R. Rice, Conditions for the localization of deformation in pressure-sensitive dilatant materials, *J. Mech. Phys. Solids, 23*, 371–394, 1975.

Wawersik, W. R., and C. Fairhurst, A study of brittle rock fracture in laboratory compression experiments, *Int. J. Rock Mech. Min. Sci., 7*, 561–575, 1970.

Wawersik, W. R., J. W. Rudnicki, W. A. Olsson, D. J. Holcomb, and K. T. Chau, Localization of deformation in brittle rock: theoretical and laboratory investigations, in *Micromechanics of Failure of Quasi-brittle Materials*, edited by S. P. Shah, S. E. Swartz, and M. L. Wang, Elsevier Applied Science, New York, 115–124, 1990.

Wong, T.-F., H. Szeto, and J. Zhang, Effect of loading path and porosity on the failure mode of porous rocks, *Appl. Mech. Rev., 45*, 281–293, 1992.

W. A. Olsson, Geomechanics Department, Sandia National Laboratories, MS 0751, Albuquerque, NM 87185-0751. (e-mail: waolsso@sandia.gov)

This preprint was prepared with AGU's LaTeX macros v4. File Luders formatted March 16, 1999.